Depletion Forces Drive Reversible Capture of Live Bacteria on Non-adhesive Surfaces

Wuqi Amy Niu,[1] Sylvia L. Rivera,[2] M. Sloan Siegrist,[2,3] and Maria M. Santore[1,3*]

1. Department of Polymer Science and Engineering, University of Massachusetts, Amherst, MA 01003
2. Department of Microbiology, University of Massachusetts, Amherst, MA 01003
3. Molecular and Cellular Biology Graduate Program, University of Massachusetts, Amherst, MA 01003

*corresponding author: Maria Santore
Department of Polymer Science and Engineering
University of Massachusetts
120 Governors Drive
Amherst, MA 01003
413-577-1417
santore@mail.pse.umass.edu

Abstract

Because bacterial adhesion to surfaces is associated with infections and biofilm growth, it has been a longstanding goal to develop coatings that minimize biomolecular adsorption and eliminate bacteria adhesion. We demonstrate that, even on carefully-engineered non-bioadhesive coatings such as polyethylene glycol (PEG) layers that prevent biomolecule adsorption and cell adhesion, depletion interactions from non-adsorbing polymer in solution (such as 10K PEG or 100K PEO) can cause adhesion and retention of *Escherichia coli* cells, defeating the antifouling functionality of the coating. The cells are immobilized and remain viable on the timescale of the study, at least up to 45 minutes. When the polymer solution is replaced by buffer, cells rapidly escape from the surface, consistent with expectations for the reversibility of depletion attractions. The dissolved polymer additionally causes cells to aggregate in solution and aggregates rapidly dissociate to singlets upon tenfold dilution in buffer, also consistent with depletion. Hydrodynamic forces can substantially reduce the adhesion of aggregates on surfaces in conditions where single cells adhere via depletion. The findings reported here suggest that because bacteria thrive in polymer-rich environments both *in-vivo* and *in-situ*, depletion interactions may make it impossible to avoid bacterial retention on surfaces.

Keywords: bacterial adhesion, cell adhesion, aggregation, entropic forces, polymer interactions

Introduction

The attachment of bacterial cells to surfaces is the first step of biofilm formation and the establishment of infections.[1, 2] Upon surface attachment, cells undergo changes in gene expression that increase virulence,[3] antibiotic tolerance,[4] and produce phenotypic changes associated with the biofilm itself.[5-9] Attachment is typically attributed to physicochemical interactions (electrostatic, hydrophobic, hydrogen bonding and other donor-acceptor) between a bacterial cell and the surface, either directly with the exposed surface chemistry or with an overlayer of adsorbed biomolecules (proteins and other entities), or fouling species.[7]

Avoiding bacterial adhesion is a goal in many different technology sectors for a variety of surfaces, only a small fraction of which are implanted in the body. However, it is interesting that biocompatible coatings, especially those of polyethylene glycol, can prevent physicochemical adhesion in *in-vitro* assays, but support biofilm formation and infection *in-situ* or *in-vivo*.[10-16] Plausible explanations include physical compromise of the surface or eventual chemical degradation. Another explanation for bacterial adhesion *in-situ* on non -sticky surfaces is the presence of dissolved polymers, surfactant micelles, and nanoparticles, all of which can give rise to attractive depletion forces.

Depletion occurs when, rather than adsorbing, solvated species or "depletants" are excluded from surfaces such as those of colloidal particles. Then, when two particles approach sufficiently closely that the depletant is excluded from the gap between their surfaces, the osmotic pressure from the bulk solution drives the particles together.[17, 18] Seen from the entropic standpoint, there

are greater available configurations when the surfaces are positioned closely, leaving more surrounding volume to be occupied by the solvated species. Hence these forces also act on large surfaces and at walls.[19, 20] The range of depletion forces is set by the approximate size of the solvated species which produces a depletion zone around particles and surfaces. The strength of depletion attractions is proportional to the osmotic pressure of the depletant.[21] Thus osmotic forces increase with depletant concentration in dilute solution, eventually causing aggregation, and when suspensions are sufficiently concentrated, phase transitions.[22, 23]

In some cases, depletion forces arise when a surface is saturated by an adsorbing species, and excess of that species in solution acts as a depletant. This requires that surface saturation occur without bridging aggregation so that the suspension is fundamentally stable prior to the imposition of depletion attractions. Thus both adsorbing and depleted polymers can produce aggregation;[24, 25] however, a distinguishing feature of depletion aggregation is that it occurs above concentrations that would give aggregation through polymer adsorption. Particles aggregated by depletion can typically be resuspended upon dilution,[26] a behavior distinct from adsorption-driven aggregates that form and persist in very dilute solutions.

While depletion forces have been understood to occur in colloidal suspensions for more than half a century, their occurrence in the biological world is a recent realization.[27-31] Depletion aggregation of motile (swimming) cells such as *Escherichia coli* (*E. coli*) has formed the basis for fascinating discoveries in active matter, such as swimming and rotating aggregates, and a shifted phase transition for swimming cells compared with nonmotile controls.[32-34] Relevant to medical applications, depletion-aggregated *E. coli* were found to exhibit increased antibiotic

tolerance.[35] Notably, this route to reduce the effectiveness of antibiotics differs from transport-related challenges of delivering antibiotics to the cells near the center of aggregates. Aggregation occurs when there are sufficient numbers of cells that they find each other through collision and studies of phase separation in bacteria are typically conducted at high cell concentrations.[34]

We hypothesize that even without aggregation, depletion forces can trap bacteria against otherwise non-adhesive surfaces, potentially rendering them susceptible to the same effects seen in aggregates. This paper explores the adhesion of a flagella-free strain of *E. coli* on the walls of a flow channel that have been coated with a layer of end-tethered polyethylene glycol, confirmed for each individual experiment to prevent cell capture and adhesion. Upon introduction of a non-adsorbing poly(ethyleneglycol) (PEG) depletant, the capture of living *E. coli* on the channel wall is reported in real time. Key features of depletion-driven capture of bacteria on walls are demonstrated: concurrent cell aggregation and adhesion to chamber walls, selective capture of individual cells rather than aggregates on walls as a result of hydrodynamic forces and slower aggregate diffusion, and the reversibility of capture and aggregation when the depletant is removed or diluted.

Materials and Methods

Bacterial Cultivation and Characterization. *ΔflhD E. coli* JW1881 was purchased from the Coli Genetic Stock Center (New Haven, CT). This strain is a genetic knockout of the *flhD* gene and does not grow flagellae. The lack of flagella was confirmed via electron microscopy and the lack of motility was confirmed in motility plate assays.[36]

E. coli were grown overnight at 37ºC in lysogeny broth (LB). To remove residual proteins and other macromolecular constituents, cells were washed three times with phosphate-buffered saline (PBS: 0.008M Na_2HPO_4, 0.002M KH_2PO_4, and 0.15 M NaCl) before resuspending in the same. For all bacteria flow experiments, the resuspended cells were used within 1 h of preparation. Viability screening with propidium iodide (Sigma-Aldrich, excitation/emission at 535 nm/617 nm) before and after flow experiments (including suspended and captured cells) confirmed that the bacteria maintained viability throughout all experimental procedures.

Drops of the *E. coli* suspension were imaged at 100x in phase contrast and analyzed via Oufti[37] using the cell detection analysis tool to determine the length and width of each cell. Between 500 and 800 cells were analyzed for each of three suspensions grown on separate days, for a total of 1860 cells analyzed. For the cells in this study, which were in stationary phase, the average length was 1.8850 ± 0.0483 μm, and the average width was 0.9622 ± 0.0500 μm, where the error represents a standard deviation. From these measurements the average cell volume was estimated, as described in the Supporting Information to be 1.1356 μm^3. This approximate

volume was employed in estimates of the cell volume fraction for different cell number concentrations, also described in the Supporting Information.

Non-Bioadhesive Surfaces. To create surfaces that were not adhesive to cells, to poly(ethylene glycol) (PEG), or to poly(ethylene oxide) (PEO), microscope slides were modified with an end-tethered PEG coating. Microscope slides (Fisher finest) were first soaked overnight in concentrated sulfuric acid and then rinsed thoroughly with deionized water and dried under nitrogen. After sealing an acid etched slide in the laminar slit flow chamber, it was filled with flowing PBS. Then a 100 ppm solution of PEG-poly-L-lysine (PEG-PLL) copolymer was flowed at a wall shear rate of 22 s^{-1} over the surface for 10 minutes, after which PBS flow was resumed. The time of PEG-PLL solution flow was determined to be more than needed to saturated the surface.[38] The coated surface was then employed directly in depletion studies without opening the flow chamber.

The PLL-PEG copolymer itself was synthesized as previously described,[38-40] using a PLL having a nominal molecular weight of 15,000-30,000 g/mol from Sigma and methoxypoly(ethylene glycol)-succinimidyl valerate (mPEG-SVA) with a nominal molecular weight of 5,000 g/mol from Laysan Bio Inc. The amines of the PLL were approximately 30% functionalized with PEG side chains, to produce a graft copolymer that adsorbs by its main PLL backbone to acid etched microscope slides with the PEG side chains extending into solution. In this manner PLL-PEG adsorption produces an end-tethered PEG coating with well-established resistance to protein and cell adhesion.[11, 39, 41-43] In our hands, adsorbed layers of PEG-PLL copolymers having the specific architecture employed here did not adsorb detectible amounts of fibrinogen and

albumin.[38, 44] They also prevented the accumulation of *E. coli*,[36] *Staphylococcus aureus*,[45-48] and Jurkat and MCF-7 cells[49] in our lab, but they were displaced by polycation homopolymers.[50] Studies in the supporting information, employing a near-Brewster optical reflectometer[51] demonstrate that PEG chains from solution do not displace or adsorb onto established PLL-PEG layers.

Bacteria Capture Studies. In studies of bacteria capture, a laminar-slit flow chamber, containing a PEG-modified observation window, was mounted in a custom-built lateral optical microscope with a 20x Nikon objective. This apparatus orients the test surface perpendicular to the optical bench so that gravity does not act normal to the surface. In step 1, after flowing PBS, *E. coli* were flowed over the surface at a wall shear rate of 8 s^{-1}. The camera, focused on the chamber wall, was used to record at least 10 minutes of video to establish a complete lack of cell capture. Step 1 ensured that the PEG layer had been established effectively and that the surface was not fundamentally adhesive towards *E. coli* cells.

Next in step 2, a PEG solution was quickly mixed with fresh bacterial suspension to give a cell concentration of 1.3 x10^8 cells/mL (having cell volume fraction, ϕ_{cell} = 1.5 x 10^{-4}, as described in the Supporting Information) and the desired concentration of PEG or PEO depletant in the feed reservoir. The depletant was molecular weight standard 10,370 g/mol PEG, with a polydispersity of 1.04, or molecular weight standard 85,200 g/mol poly(ethylene oxide) (PEO) with a polydispersity of 1.07, from Agilent Technologies. Based on light scattering, Devanand and Selser[52] report a dependence of R_g on PEO molecular weight $R_g = 0.02\ MW^{0.58}\ (nm)$, which gives, for our samples, R_g = 4.2 nm and 14.5 nm for the PEO of molecular weights 10,370 g/mol

and 85,200 g/mol, respectively. These estimated R_g values are in excellent agreement with R_g for a self-avoiding chain, $R_g^{Flory} = 0.398\, a_{Flory} N^{3/5}$, where a_{Flory} depends on the Kuhn and monomer lengths in a complex manner. We employ a_{Flory} = 0.40 from a fit to molecular dynamic simulations[37] in affirming Devanand and Selser's form. These values of R_g translate to coil volumes of $\frac{4\pi}{3} R_g^3 = 310$ nm^3 and 12,770 nm^3 for the 10,370 g/mol and 85,200 g/mol samples, respectively.

The depletant-bacterial suspension was immediately pumped through the flow chamber so that the flow in the chamber was continuous, cell concentration from step 1 to step 2 was constant, and the depletant was introduced as video recording continued. After depletant and cells flowed for the desired time, flow was switched back to buffer in step 3 to probe the reversibility of cell capture. The entire process was recorded on video.

Images from video frames were analyzed by first background-subtracting a control frame prior to bacteria introduction, to remove image features from aberrations on the camera's detector array. To generate cell capture and release traces, each cell in the frame was located and counted employing a self-written Python code implementing the OpenCV library.[53] To develop images for publishable figures, time-lapse averaging of video frames was employed to clearly identify when cells were immobilized as opposed to moving. This was needed when figures are generated from individual video frames, since it is not possible for the reader to know which cells are arrested and which are flowing. In the results section, figure captions clearly state when time-lapse methods have been employed in generating a figure.

Bacteria Aggregation and Settling. In separate studies of bacteria aggregation and settling, suspensions of bacteria were mixed with PEG solutions to give a fixed final cell concentration of 6.3×10^8 cells/mL ($\phi_{cell} = 7.2 \times 10^{-4}$), and the targeted PEG concentrations. This is ~5 times higher than the concentration used in flow studies to clearly enable visualization of the suspension against a dark background. The higher concentration also enabled microscopy on aggregates and their dissociation upon 10-fold dilution. Cuvettes containing a fixed bacterial concentration and varied polymer concentrations were lined up in front of a camera to monitor settling over a 12 hour period, to evidence aggregation. In rapid assays, depletant was mixed with cells in a vial and examined at 40x in bright field to identify aggregates or dispersion of aggregates upon dilution. In a control study with an absorbing polymer, PLL (nominal molecule weight 15,000-30,000 g/mol from Sigma) was employed as the adhesive polymer.

RESULTS AND DISCUSSION

Depletion Driven Adhesion on a Flow Chamber Wall

Critical to the exploration of depletion-driven adhesion is the use of surfaces that are fundamentally non-adhesive. This is ensured here through the application of a non-adhesive layer of end-tethered 5,000 g/mol PEG chains, established previously to repel proteins and cells and to be retained during their flow.[11, 38, 39, 41, 45, 46, 49] The supporting information further demonstrates that the coating is retained upon exposure to PEG depletant which, as expected, does not adhere to or incorporate into the surface. After assembling the flow chamber and establishing the PEG brush coating on the microscope slide (the observation window), experiments probing bacterial interactions employed three steps: 1) demonstrating the non-adhesive nature of each PEG surface towards *E. coli* cells, 2) quantifying cell capture in the presence of depletant and 3) establishing the reversibility of the depletion-driven capture. It is important to note that the orientation of the flow chamber on a "lateral" microscope eliminates any impact of gravity pulling cells towards or away from the surface.

A typical run is shown in Figure 1A, with excerpted micrographs in Figures 1B-1D. In step 1, *E. coli* cells are flowed in buffer over a PEG-coated surface at a concentration of 1.3×10^8 cells/mL ($\phi_{cell} = 1.5 \times 10^{-4}$), and a wall shear rate of 8 s^{-1}. A long exposure frame in Figure 1B, illustrates that cells do not accumulate or come to rest on the PEG surface, even momentarily. They flow past the surface in the moving fluid and hence they do not appear in the long exposure image. Next, in step 2, PEO depletant is introduced by continuing to flow an *E. coli* suspension containing 1.3×10^8 cells/mL in the same buffer but now with 0.5 wt% PEO (85,200 g/mol) also in solution. This corresponds to a polymer coil volume fraction of $\phi_p = 0.45$. The wall shear rate

is kept at 8 s^{-1}. It is seen that with free PEO added to the solution, cells accumulate on the surface, growing in number with increased time, in Figure 1C. Finally in step 3, flowing buffer is reintroduced and cells come off the surface, in Figure 1D. It is important to note that during step 1, all cells were singlets, however in step 2, small aggregates (containing no more than ~10 cells) appear in the flowing fluid. Very few aggregates adhered to the surface and, when they did, they were counted as a single unit. It is also important to note that the flowing and captured cells are alive, as determined by their ability to grow and divide on the surface, a subject of ongoing study.

Figure 1A contains several interesting features which will be addressed below: During step 2 the accumulation *rate* of adhered cells decreased in time; upon reintroduction of buffer in step 3 there was a short increase in the numbers of adhered cells just before their escape from the surface; and the release of cells from the surface, once its started, occurred more rapidly than the accumulation. These kinetic features are consistent with expectations for systems experiencing depletion forces, elaborated below.

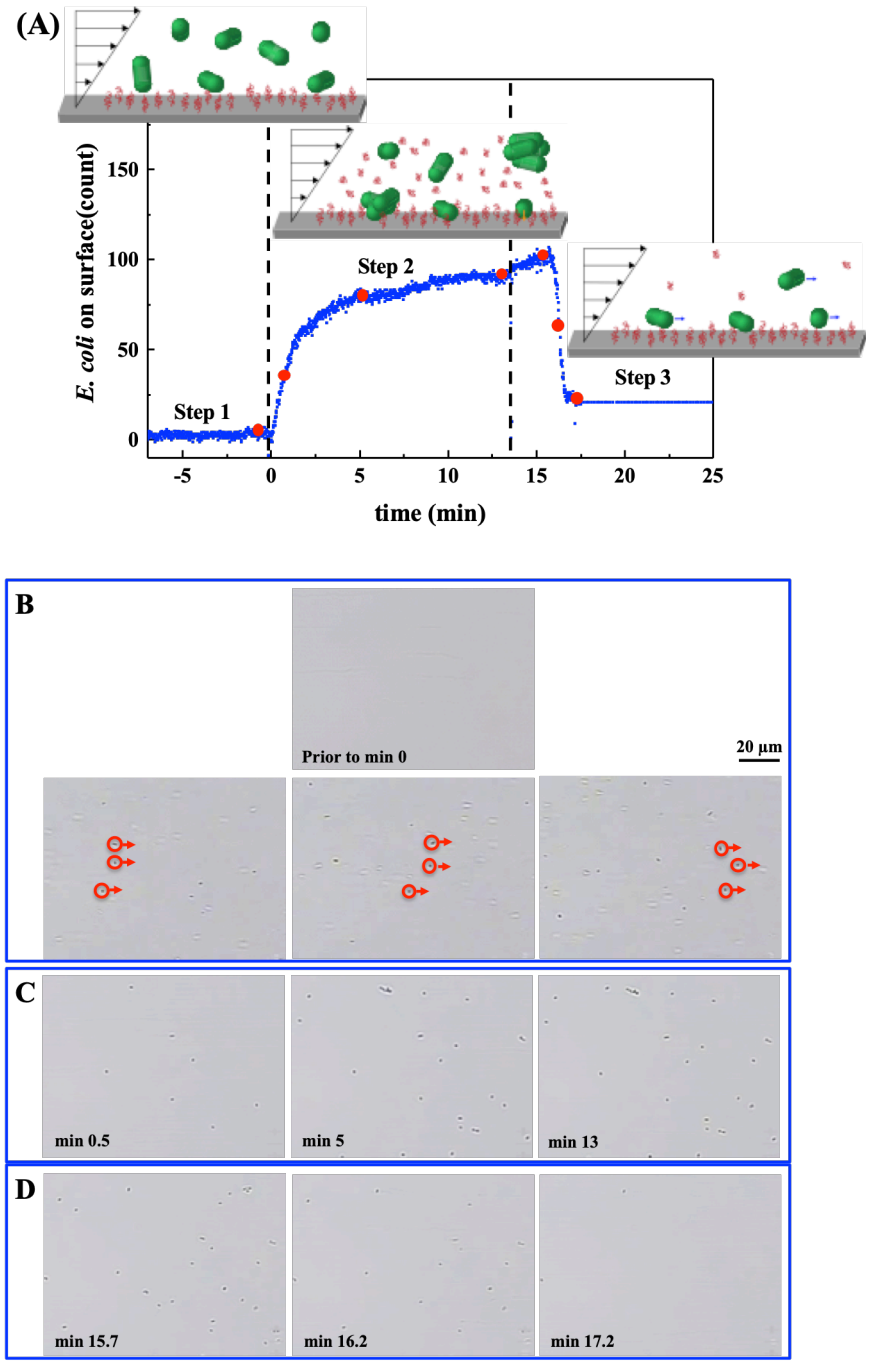

Figure 1. Capture and release of *E. coli* on a PEG surface, using 0.5 wt% 85,200 g/mol PEO depletant ($\phi_p = 0.45$). A) Counts of immobilized cells in time in the full 178 µm x 263 µm viewing window and schematics of three-step process probing 1) nonadhesive surface character with only bacteria flow 2) depletion-driven capture with flowing cells and depletant 3) reversibility of capture with only flowing buffer. B) Micrographs during flow of cells prior to PEO addition in step 1. One long-exposure frame and three standard video frames 4 seconds apart. C) Long exposure microvideo frames during cell capture in the presence of 0.5 wt% 85,200 g/mol PEO in step 2. D) Long exposure microvideo frames during reintroduction of buffer and cell release in step 3. Long exposure frames average images from 5 s of video, blurring or eliminating moving objects. Microvideo frames of 89 x 119 µm, in B-D correspond to points labeled on part A.

The general shape of the cell capture trace in Figure 1A is highly reproducible, especially the initial slope and the long time slopes of cell capture during step 2. Five runs using different bacterial batches on different days are shown in Figure 2A. The differences in the times of crossover from the fast initial slope to the slower later slope likely result from different aggregation times or amounts, sensitive to mixing technique during suspension preparation for step 2. The significance of the different kinetic regimes will be addressed below. Figure 2B additionally compares the depletion-driven capture of cells by 10,370 g/mol PEG (2 wt%, ϕ_p = 0.36) and 85,200 PEO (0.5 wt%, ϕ_p = 0.45) depletant. The different concentrations were chosen based on aggregation studies described in a later section and literature.[19, 31, 34] In Figure 2B, representative of 3 runs, a slightly lower initial slope is seen with the lower molecular weight PEG depletant. The lower slope for this concentration of the 10,370 g/mol PEG is a reproducible feature for these polymers at these concentrations, and may be a reflect weaker or shorter range attractions, as evidenced by the slippage of some cells along the surface in gentle flow at the lower molecular weight only.

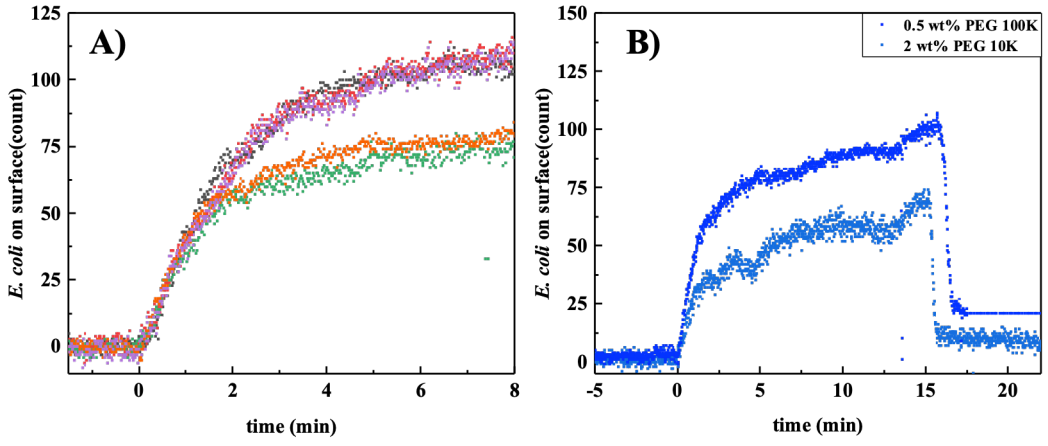

Figure 2. (A) Overlay of Steps 1 and 2 (schematic Figure 1A) from 5 different runs with different batches of *E. coli* on different days. (B) Comparison of depletion capture and release using 0.5 wt% 85,200 g/mol PEO versus 2 wt% 10,370 g/mol PEG. Cell counts correspond to the full viewing area: 178 µm x 263 µm

Evidence for the Depletion Mechanism

In the micrographs of Figure 3, dissolved PEO is seen to produce reversible aggregation in *E. coli* cell suspensions, a behavior consistent with depletion of PEO from the cell surfaces. Figure 3A shows a suspension *E. coli* cells (concentration of 6.3 x 10^8 cells/ml, $\phi_{cell} = 0.00072$) in a buffered 0.5 wt% 85,200 g/mol PEO solution ($\phi_p = 0.45$). Aggregates are visible compared with the buffer control in Figure 3B that contains only singlet cells. In Figure 3A when diluted by a factor of 10 in buffer the PEO-induced aggregates disperse and the suspension appears similar to that of the cells in buffer after 10-fold dilution. The immediate dispersion of aggregates upon dilution is consistent with depletion aggregation. By contrast, in Figure 3C a suspension containing 6.3 x 10^8 *E. coli* cells/mL ($\phi_{cell} = 0.00072$) aggregates in the presence of 0.1wt% PLL homopolymer that adsorbs to the cells via electrostatic attraction. Ten-fold dilution does not disperse the aggregated cells, demonstrating the irreversibility of aggregation by adsorbing polymer and providing a contrast to the depletion attractions resulting from PEO.

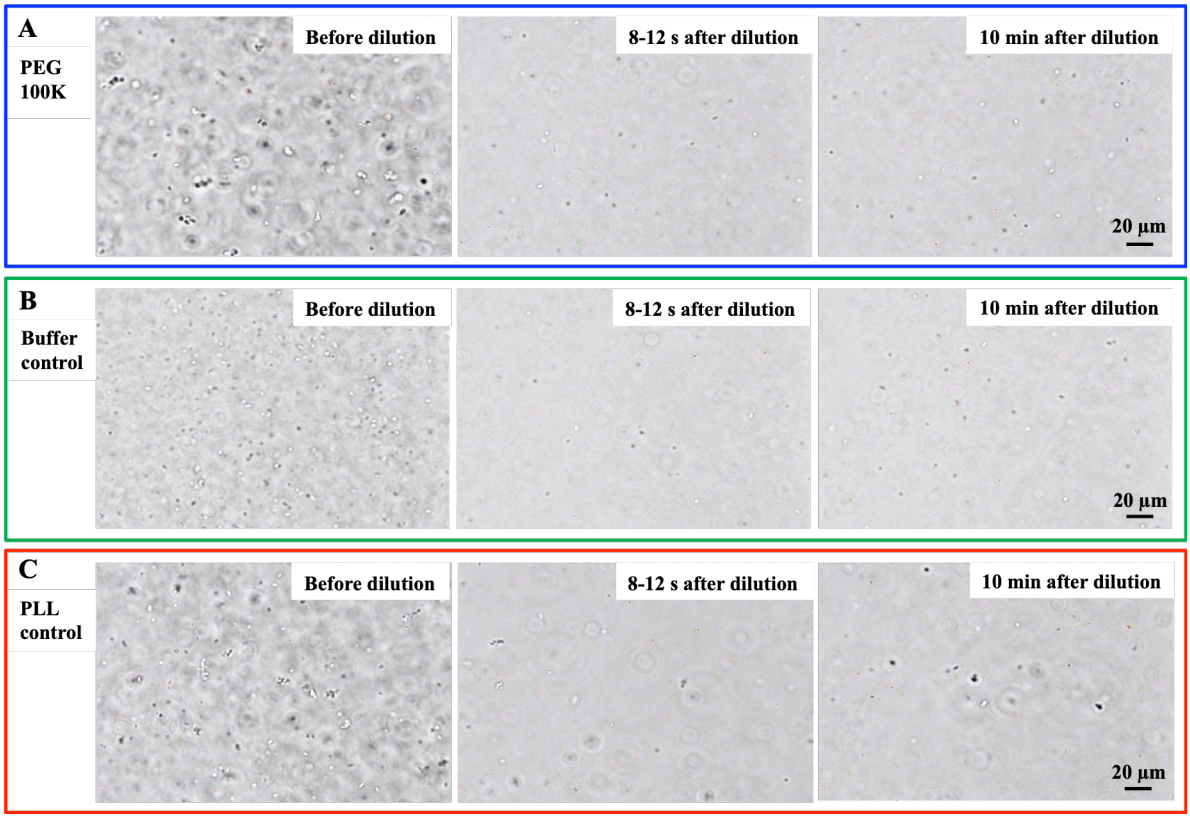

Figure 3. A) Buffered *E. coli* suspension initially containing 6.3 x 10^8 cells/mL(ϕ_{cell} = 0.00072) and (left) and 0.5 wt% PEO(ϕ_p = 0.45) having 85,200 g/mol, showing aggregation. Middle and right panels show the suspension 8-12 s and 10 minutes, respectively, after 10-fold dilution in buffer that causes cells to disperse. B) Control run showing (left) buffered *E. coli* suspension initially containing 6.3 x 10^8 cells/ml without PEG, and lacking aggregation. Middle and right panels show the suspension 8-12 s and 10 minutes, respectively, after 10-fold dilution in buffer. C) Control run showing (left) buffered *E. coli* suspension initially containing 6.3 x 10^8 cells/ml and 0.1 wt% PLL, showing aggregation. Middle and right panels show the suspension 8-12 s and 10 minutes, respectively, after 10-fold dilution in buffer, but still aggregated.

Figures 4A and B further argue for the depletant action of PEG in *E. coli* suspensions for 10,370 and 85,200 g/mol PEO, respectively. Here series of *E. coli* suspensions with a fixed cell

concentration of 6.3 x 10^8 cells /mL (ϕ_{cell} = 0.00072) and increasing concentrations of PEG or PEO exhibit different extents of settling, facilitated by the aggregation of cells driven by added polymer. The top row shows the initial appearance of the suspensions and the lower images show that settling occurs gradually in some vials over time. Minimal settling occurs without aggregation, for instance without added PEG or PEO or in the dilute limit, when the amount of added PEG or PEO is below that needed to produce depletion aggregation.

The aggregation in Figure 4 is consistent with depletion, for instance requiring relatively high polymer concentrations to aggregate a relatively dilute (ϕ_{cell} = 0.00072) bacterial suspension. The appearance of settling in the series of cuvettes, increasing sharply at a specific polymer concentration, resembles studies of depletion-driven phase transitions in bacterial[31, 34] and particulate[22, 54] systems, though with different cells or particles and different polymers a quantitative comparison should not be made. In Figure 4A, 85,200 g/mol PEG accelerates settling above about 0.1 wt% (ϕ_p = 0.09) added polymer which produces aggregation, while in Figure 4B for 10,370 g/mol PEG, this effect is seen above about 1 wt% PEG (ϕ_p = 0.18), motivating the particular polymer concentrations in the flow chamber study. The experimental results of Figure 4 are also in qualitative agreement, with a recent theoretical treatment,[55] though Figure 4 shows settling at PEO concentrations somewhat lower than predicted, potentially due to differences in polymer/cell size ratio.

Importantly, we find (in the Supporting Information) that, when the cell concentration (6.3 x 10^9 cells/ml, ϕ_{cell} = 0.0072) is an order of magnitude higher than in Figure 4, settling starts to occur at polymer concentrations of 0.05 wt% PEO (ϕ_p = 0.045), or 1 wt% PEG (ϕ_p = 0.18). The trend

that similar or slightly lower polymer concentration is required to aggregate or phase separate suspensions of increasing concentration is a key signature of depletion[31, 54-56] and is opposite that seen aggregation by adherent polymer. This suggests that the aggregation and settling of Figure 4 are the initial kinetic steps toward phase separation and equilibration between cell-dense and cell-sparse phases. Most import for cell-wall interactions, the exercise in Figure 4 demonstrates that cells are subject to depletion forces from PEO and PEG.

A separate point of interest, Figure 4A shows that for the 85,200 g/mol PEG, settling is not seen above about 2 wt% PEG. This may be a result of depletion driven gelation at high polymer concentrations, reported by some.[57, 58] Alternatively it may result from depletion forces of decreasing range above c*, which occurs at about 1 wt% for this molecular weight. As polymer chains become increasingly concentrated in solution so that their coils overlap, the lengthscale of depletion forces decreases,[59] allowing stabilizing mechanisms such electrostatic repulsion to play an increasing role and ultimately eliminate the phase transition.[60] The overlap concentration is not approached in Figure 4B for the 10,370 g/mol molecular weight.

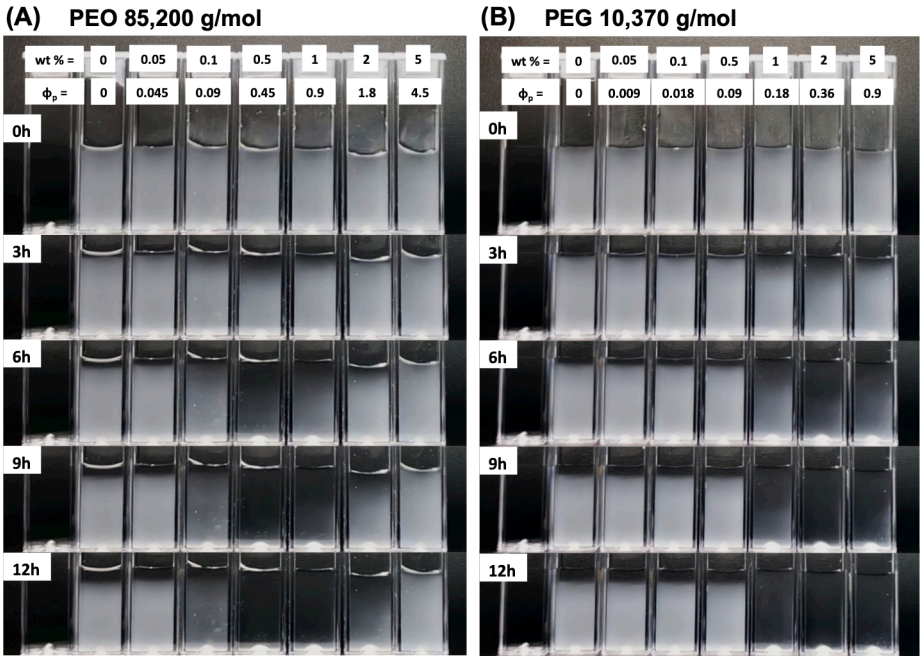

Figure 4. Depletion of (A) PEO and (B) PEG produces aggregates that settle to form a dense phase in *E. coli* suspensions containing 6.3 x 10^8 cells/mL (ϕ_{cell} = 0.00072). The times are indicated on the labels on the left side of each series. The depletant concentrations in polymer wt% and polymer coil volume fraction are indicated on the labels across the top. The left most cuvette in each series contains only buffer.

Depletion Adhesion versus Depletion-driven Aggregation

Cell aggregation, established in Figures 3 and 4, competes with cell adhesion to a wall and is responsible for some of the features in the kinetic traces of Figure 1A and 2. During step 2, aggregation occurs in the bulk solution of the flow chamber and in the feed reservoir, progressively reducing the concentration of free cells on timescales of minutes, shown in the

Supporting Information. We find that despite the presence of these aggregates and the capture of a few of them, adherent cells are primarily singlets (for instance in Figure 1C). This is likely due to the greater hydrodynamic forces on aggregates relative to single cells, scaling roughly as the square of the size of the object, either cell or aggregate. Thus progressive aggregation reduces the numbers of single cells available during step 2, so that the rate of cell capture decreases from its initially rapid kinetics before the surface is saturated. Indeed, in studies of the capture of rod shaped colloids similar in size and shape to *E. coli*,[61] rapid transport limited capture on electrostatically-attracting surfaces was found to proceed to beyond 3-4 times the surface loadings compared with the slower capture is observed in Figures 1A and 2. Thus the rate reduction of depletion aggregation occurs due to factors other than surface saturation or hydrodynamic blocking of approaching cells by those already on the surface.

The initial fast cell capture in step 2 of Figure 1A and 2 is due to adhesion of singlets to wall. We hypothesize, however, that the rapidly captured cells are those already present in the flow chamber in buffer (from step 1) and that they are forced to the wall by the free PEG or PEO that is introduced in step 2, before the original cells have time to aggregate. The free PEG or PEO must reach the wall at the observation point far more quickly than the newly introduced cells (and aggregates) with which they are mixed only minutes in advance. This is the case because PEG or PEO coils are orders of magnitude smaller and diffuse proportionately faster than cells and aggregates.

To test this mechanism, we compared different protocols to introduce cells and depletant in Figure 5. The blue data follow a protocol for steps 1 and 2 of Figure 1, where cells are initially

flowing over a surface and a PEG-containing suspension is added, keeping the cell concentration in the bulk solution fixed, but introducing PEO depletant. The green data are produced in a run that starts with the flow of buffered *E. coli* (step 1), and then a PEO solution not containing *E. coli* is introduced. Cells are removed from the bulk solution as the PEO solution is introduced; however as the cells are flushed away, those in near-wall region are captured on the wall. Then, even though no cells remain in bulk solution after a few minutes, the depletion forces from the PEO hold the cells captured against the wall. The lack of cells in the bulk solution (the absence of new cells being introduced) causes the green data set to be flat at long times. The red data set illustrates that without cells present in the chamber in advance, the introduction of a PEO-containing suspension produces only slow capture of new cells. Overall, the initial rapid rise in adhered cells is seen in runs where free cells are present in advance of the PEO introduction. The continued rise at long times (which is of similar slope in the red and blue runs) occurs when PEO and bacteria are present in the bulk solution.

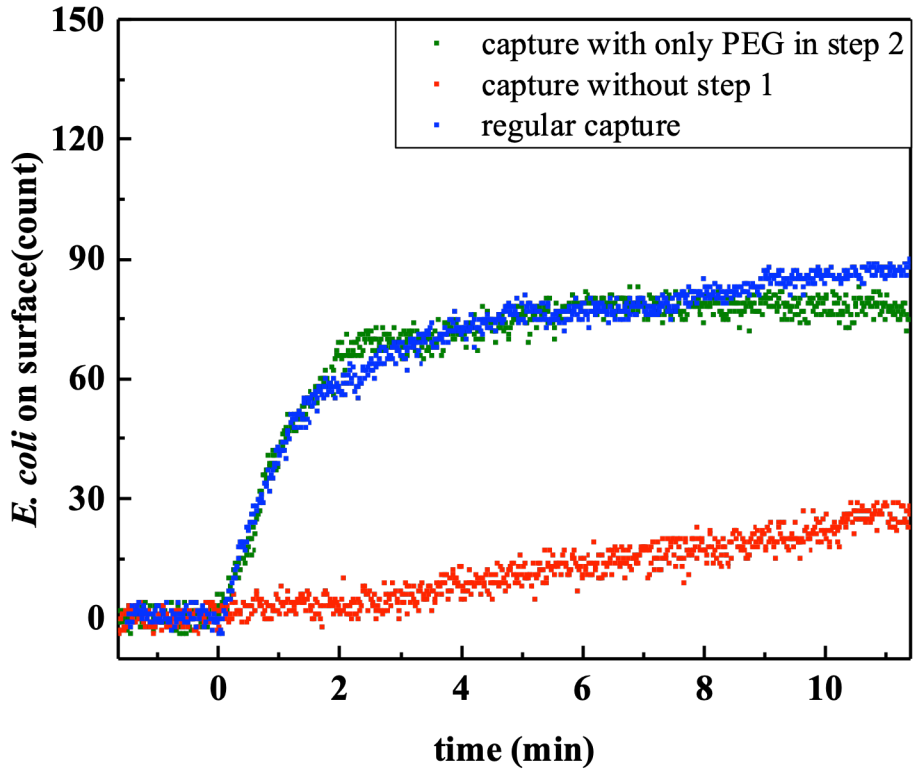

Figure 5. Three runs comparing features of depletion-driven capture using 0.5 wt% 100K PEG depletant. Blue run starts with free cells in chamber, flowing over surface (step 1 of Figure 1A) and subsequent injection of bacterial suspension with PEO added. The green run also starts with cells flowing past the surface in buffer, followed by the introduction of 0.5 wt% 85,200 g/,mol PEO depletant not containing cells. The red run shows cell capture when a newly mixed suspension of *E. coli* and PEO is introduced into the flow chamber after buffer flow (but with no prior flow of a buffered *E. coli* suspension). Cell counts correspond to the full viewing area: 178 μm x 263 μm

Cell Release

A final interesting feature of the depletion-driven capture, in Figures 1A and 2B, is the rapid and near complete release of cells upon removal of the depletant. The release occurs quickly once the local PEG or PEO concentration within a micron of the wall drops below that needed to produce sufficient depletion force. Because the cell-wall attraction is "turned off" all at once (on

the timescale of PEG or PEO diffusion in the near wall gradient produced by shear flow), the cell release occurs abruptly. Free cells are carried away by flow, without needing to diffuse substantially perpendicular the surface. The near complete release of the cells evidences the underlying non-adhesive character of the PEG brush which appears not to be compromised by squeezing contact with the cells at these timescales. It is interesting to note, in Figure 6, that we sometimes do see adhered aggregates on the order of 5-6 cells. Upon removal of depletant, these aggregates sometimes disperse as they come off the surface. Other times, the entire aggregate is disengaged from the surface. The difference is likely in the cell-cell interactions and is beyond the current scope.

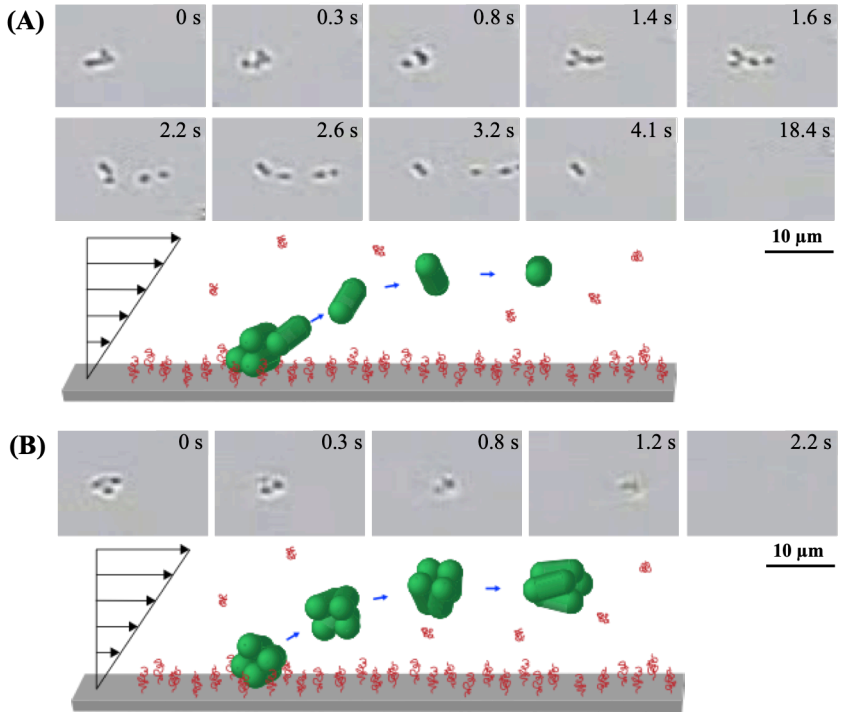

Figure 6. Release of aggregates upon reintroduction of buffer. (A) Aggregate disperses (B) entire aggregate is released at once. Times are shown relative to a first frame prior to release.

Conclusions

This study demonstrated that depletion forces can trap live bacterial cells on otherwise non-adhesive surfaces even in gentle and flow and when the surfaces are oriented so that capture is not aided by gravitational settling of cells. Capture is reversible and, due to the non-adhesive underlying nature of the surface, captured cells escape quickly when depletant is removed. When bacterial suspensions are present near a surface, introduction of depletant can cause cell adhesion that is more rapid than exposure of a surface containing both bacterial cells and polymer. The polymer concentrations producing cell capture on surfaces are similar to those causing aggregation in solution. As a result aggregation can compete with cell capture on a wall. Even with gentle flow, depletion forces produce a preference for the capture of single cells rather than aggregates, ensuring contact of captured cells with a surface. Since the cells remain alive during depletion adhesion, their capture may promote biofilm formation and infection. Bacterial replication under this condition is the subject of ongoing study. Thus depletion-driven adhesion provides a mechanism for the adhesion of cells to otherwise non-adhesive engineered surfaces in polymer-rich environments.

Acknowledgments. This work was supported by NSF 1848065. We thank Dr. Mark Tuominen and Dr. Zhou Xu for their valuable input and Ms. Rebecca Gordon for additional cell preparations during the manuscript revision.

References

1. Donlan, R. M. Biofilms: Microbial life on surfaces. *Emerg. Infect. Dis* **2002**, *8*, 881-890.

2. Donlan, R. M.; Costerton, J. W. Biofilms: Survival mechanisms of clinically relevant microorganisms. *Clin. Microbiol. Rev.* **2002**, *15*, 167-+.

3. McCarter, L.; Hilmen, M.; Silverman, M. Flagellar Dynomometer Controls Swarmer Cell-Differentiation of V-Parahaemolyticus. *Cell* **1988**, *54*, 345-351.

4. Olsen, I. Biofilm-specific antibiotic tolerance and resistance. *Eur. J. Clin. Microbiol. Infect. Dis.* **2015**, *34*, 877-886.

5. Hodl, I.; Hodl, J.; Worman, A.; Singer, G.; Besemer, K.; Battin, T. J. Voronoi Tessellation Captures Very Early Clustering of Single Primary Cells as Induced by Interactions in Nascent Biofilms. *PLoS One* **2011**, *6*.

6. Irvine, S.; Bunk, B.; Bayes, H. K.; Sproer, C.; Connolly, J. P. R.; Six, A.; Evans, T. J.; Roe, A. J.; Overmann, J.; Walker, D. Genomic and transcriptomic characterization of Pseudomonas aeruginosa small colony variants derived from a chronic infection model. *Microb. Genomics* **2019**, *5*.

7. Rice, A. R.; Hamilton, M. A.; Camper, A. K. Apparent surface associated lag time in growth of primary biofilm cells. *Microb. Ecol.* **2000**, *40*, 8-15.

8. Sauer, K.; Camper, A. K. Characterization of phenotypic changes in Pseudomonas putida in response to surface-associated growth. *J. Bacteriol.* **2001**, *183*, 6579-6589.

9. Yang, L.; Jelsbak, L.; Marvig, R. L.; Damkiaer, S.; Workman, C. T.; Rau, M. H.; Hansen, S. K.; Folkesson, A.; Johansen, H. K.; Ciofu, O.; Hoiby, N.; Sommer, M. O. A.; Molin, S. Evolutionary dynamics of bacteria in a human host environment. *Proc. Natl. Acad. Sci. U. S. A.* **2011**, *108*, 7481-7486.

10. Carnt, N. A.; Evans, V. E.; Naduvilath, T. J.; Willcox, M. D. P.; Papas, E. B.; Frick, K. D.; Holden, B. A. Contact Lens-Related Adverse Events and the Silicone Hydrogel Lenses and Daily Wear Care System Used. *Archives of Ophthalmology* **2009**, *127*, 1616-1623.

11. Harris, L. G.; Tosatti, S.; Wieland, M.; Textor, M.; Richards, R. G. Staphylococcus aureus adhesion to titanium oxide surfaces coated with non-functionalized and peptide-functionalized poly(L-lysine)-grafted-poly(ethylene glycol) copolymers. *Biomaterials* **2004**, *25*, 4135-4148.

12. Wang, Y.; Guan, A.; Isayeva, I.; Vorvolakos, K.; Das, S.; Li, Z. Y.; Phillips, K. S. Interactions of Staphylococcus aureus with ultrasoft hydrogel biomaterials. *Biomaterials* **2016**, *95*, 74-85.

13. Willcox, M. D. P.; Harmis, N.; Cowell, B. A.; Williams, T.; Holden, B. A. Bacterial interactions with contact lenses; effects of lens material, lens wear and microbial physiology. *Biomaterials* **2001**, *22*, 3235-3247.

14. Funt, D.; Pavicic, T. Dermal Fillers in Aesthetics: An Overview of Adverse Events and Treatment Approaches. *Clin. Cosmet. Investig. Dermatol.* **2013**, *6*, 295-316.

15. Romano, C. L.; Tsuchiya, H.; Morelli, I.; Battaglia, A. G.; Drago, L. Antibacterial coating of implants: are we missing something? *Bone Jt. Res.* **2019**, *8*, 199-205.

16. Wang, M. Q.; Tang, T. T. Surface treatment strategies to combat implant-related infection from the beginning. *J. Orthop. Transl.* **2019**, *17*, 42-54.

17. Asakura, S.; Oosawa, F. On Interactions between 2 Bodies Immersed in a Solution of Macromolecules. *J. Chem. Phys.* **1954**, *22*, 1255-1256.

18. Asakura, S.; Oosawa, F. Interaction between Particles Suspended in Solutions of Macromolecules. *Journal of Polymer Science* **1958**, *33*, 183-192.

19. Nam, J.; Santore, M. M. Depletion versus Deflection: How Membrane Bending Can Influence Adhesion. *Phys. Rev. Lett.* **2011**, *107*.

20. Ji, S. X.; Walz, J. Y. Depletion forces and flocculation with surfactants, polymers and particles - Synergistic effects. *Curr. Opin. Colloid Interface Sci.* **2015**, *20*, 39-45.

21. Evans, E. A. Force between Surfaces that Confine a Polymer Solution - Derivation from Self-Consistent Field Theories *Macromolecules* **1989**, *22*, 2277-2286.

22. Gast, A. P.; Hall, C. K.; Russel, W. B. Polymer-Induced Phase Separations in Non-aqueous Colloidal Suspensions *J. Colloid Interface Sci.* **1983**, *96*, 251-267.

23. Gast, A. P.; Russel, W. B.; Hall, C. K. An Experimental and Theoretical Study of Phase Transitions in the Polystyrene Latex and Hydroxyethylcellulose System *J. Colloid Interface Sci.* **1986**, *109*, 161-171.

24. Santore, M. M.; Russel, W. B.; Prudhomme, R. K. Experimental and Theoretical Study of Phase Transitions Indcued in Colloidal Dipsersions by Associative Polymers. *Faraday Discuss.* **1990**, *90*, 323-333.

25. Santore, M. M.; Russel, W. B.; Prudhomme, R. K. A 2-COMPONENT MODEL FOR THE PHASE-BEHAVIOR OF DISPERSIONS CONTAINING ASSOCIATIVE POLYMER. *Macromolecules* **1989**, *22*, 1317-1325.

26. Poon, W. C. K. The physics of a model colloid-polymer mixture. *J. Phys.-Condes. Matter* **2002**, *14*, R859-R880.

27. Dorken, G.; Ferguson, G. P.; French, C. E.; Poon, W. C. K. Aggregation by depletion attraction in cultures of bacteria producing exopolysaccharide. *J. R. Soc. Interface* **2012**, *9*, 3490-3502.

28. Girard, M.; Schaffer-Lequart, C. Gelation of skim milk containing anionic exopolysaccharides and recovery of texture after shearing. *Food Hydrocolloids* **2007**, *21*, 1031-1040.

29. Eboigbodin, K. E.; Newton, J. R. A.; Routh, A. F.; Biggs, C. A. Role of nonadsorbing polymers in bacterial aggregation. *Langmuir* **2005**, *21*, 12315-12319.

30. Porter, M. K.; Steinberg, A. P.; Ismagilov, R. F. Interplay of motility and polymer-driven depletion forces in the initial stages of bacterial aggregation. *Soft Matter* **2019**, *15*, 7071-7079.

31. Schwarz-Linek, J.; Winkler, A.; Wilson, L. G.; Pham, N. T.; Schilling, T.; Poon, W. C. K. Polymer-induced phase separation in Escherichia coli suspensions. *Soft Matter* **2010**, *6*, 4540-4549.

32. Cates, M. E.; Marenduzzo, D.; Pagonabarraga, I.; Tailleur, J. Arrested phase separation in reproducing bacteria creates a generic route to pattern formation. *Proc. Natl. Acad. Sci. U. S. A.* **2010**, *107*, 11715-11720.

33. Schwarz-Linek, J.; Valeriani, C.; Cacciuto, A.; Cates, M. E.; Marenduzzo, D.; Morozov, A. N.; Poon, W. C. K. Phase separation and rotor self-assembly in active particle suspensions. *Proc. Natl. Acad. Sci. U. S. A.* **2012**, *109*, 4052-4057.

34. Schwarz-Linek, J.; Dorken, G.; Winkler, A.; Wilson, L. G.; Pham, N. T.; French, C. E.; Schilling, T.; Poon, W. C. K. Polymer-induced phase separation in suspensions of bacteria. *Epl* **2010**, *89*.

35. Secor, P. R.; Michaels, L. A.; Ratjen, A.; Jennings, L. K.; Singh, P. K. Entropically driven aggregation of bacteria by host polymers promotes antibiotic tolerance in Pseudomonas aeruginosa. *Proc. Natl. Acad. Sci. U. S. A.* **2018**, *115*, 10780-10785.

36. Shave, M.; Xu, Z.; Raman, V.; Kalasin, S.; Tuominen, M. T.; Forbes, N. S.; Santore, M. M. Eschericia coli Swimming back Towards Stiffer Polyethylene Glycol Coatingss, Increasing Contact in Flow. *ACS Appl. Mater. Interfaces* **2021**, *doi.org/10.1021/acsami.1c00245*.

37. Liese, S.; Gensler, M.; Krysiak, S.; Schwarzl, R.; Achazi, A.; Paulus, B.; Hugel, T.; Rabe, J. P.; Netz, R. R. Hydration Effects Turn a Highly Stretched Polymer from an Entropic into an Energetic Spring. *ACS Nano* **2017**, *11*, 702-712.

38. Gon, S.; Bendersky, M.; Ross, J. L.; Santore, M. M. Manipulating Protein Adsorption using a Patchy Protein-Resistant Brush. *Langmuir* **2010**, *26*, 12147-12154.

39. Huang, N. P.; Michel, R.; Voros, J.; Textor, M.; Hofer, R.; Rossi, A.; Elbert, D. L.; Hubbell, J. A.; Spencer, N. D. Poly(L-lysine)-g-poly(ethylene glycol) layers on metal oxide surfaces: Surface-analytical characterization and resistance to serum and fibrinogen adsorption. *Langmuir* **2001**, *17*, 489-498.

40. Kenausis, G. L.; Voros, J.; Elbert, D. L.; Huang, N. P.; Hofer, R.; Ruiz-Taylor, L.; Textor, M.; Hubbell, J. A.; Spencer, N. D. Poly(L-lysine)-g-poly(ethylene glycol) layers on metal oxide surfaces: Attachment mechanism and effects of polymer architecture on resistance to protein adsorption. *J. Phys. Chem. B* **2000**, *104*, 3298-3309.

41. Dalsin, J. L.; Lin, L. J.; Tosatti, S.; Voros, J.; Textor, M.; Messersmith, P. B. Protein resistance of titanium oxide surfaces modified by biologically inspired mPEG-DOPA. *Langmuir* **2005**, *21*, 640-646.

42. Schuler, M.; Owen, G. R.; Hamilton, D. W.; De Wilde, M.; Textor, M.; Brunette, D. M.; Tosatti, S. G. P. Biomimetic modification of titanium dental implant model surfaces using the RGDSP-peptide sequence: A cell morphology study. *Biomaterials* **2006**, *27*, 4003-4015.

43. Csucs, G.; Michel, R.; Lussi, J. W.; Textor, M.; Danuser, G. Microcontact printing of novel co-polymers in combination with proteins for cell-biological applications. *Biomaterials* **2003**, *24*, 1713-1720.

44. Gon, S.; Santore, M. M. Single Component and Selective Competitive Protein Adsorption in a Patchy Polymer Brush: Opposition between Steric Repulsions and Electrostatic Attractions. *Langmuir* **2011**, *27*, 1487-1493.

45. Fang, B.; Gon, S.; Nusslein, K.; Santore, M. M. Surfaces for Competitive Selective Bacterial Capture from Protein Solutions. *ACS Appl. Mater. Interfaces* **2015**, *7*, 10275-10282.

46. Fang, B.; Gon, S.; Park, M.; Kumar, K. N.; Rotello, V. M.; Nusslein, K.; Santore, M. M. Bacterial adhesion on hybrid cationic nanoparticle-polymer brush surfaces: Ionic strength tunes capture from monovalent to multivalent binding. *Colloid Surf. B-Biointerfaces* **2011**, *87*, 109-115.

47. Gon, S.; Kumar, K. N.; Nusslein, K.; Santore, M. M. How Bacteria Adhere to Brushy PEG Surfaces: Clinging to Flaws and Compressing the Brush. *Macromolecules* **2012**, *45*, 8373-8381.

48. Kolewe, K. W.; Kalasin, S.; Shave, M.; Schiffman, J. D.; Santore, M. M. Mechanical Properties and Concentrations of Poly(ethylene glycol) in Hydrogels and Brushes Direct the Surface Transport of Staphylococcus aureus. *ACS Appl. Mater. Interfaces* **2019**, *11*, 320-330.

49. Kalasin, S.; Browne, E. P.; Arcaro, K. F.; Santore, M. M. Surfaces that Adhesively Discriminate Breast Epithelial Cell Lines and Lymphocytes in Buffer and Human Breast Milk. *ACS Appl. Mater. Interfaces* **2019**, *11*, 16347-16356.

50. Gon, S.; Fang, B.; Santore, M. M. Interaction of Cationic Proteins and Polypeptides with Biocompatible Cationically-Anchored PEG Brushes. *Macromolecules* **2011**, *44*, 8161-8168.

51. Fu, Z. G.; Santore, M. M. Poly(ethylene oxide) adsorption onto chemically etched silicates by Brewster angle reflectivity. *Colloid Surf. A-Physicochem. Eng. Asp.* **1998**, *135*, 63-75.

52. Devanand, K.; Selser, J. C. Asymptotic Behavior and Long-Range Interactions in Aqueous Solutions of Poly(ethylene oxide). *Macromolecules* **1991**, *24*, 5943-5947.

53. Van Rossum, G.; Drake, F. L., *Python 3 Reference Manual*. CreateSpace: Scotts Valley, CA, 2009.

54. Ramakrishnan, S.; Fuchs, M.; Schweizer, K. S.; Zukoski, C. F. Entropy driven phase transitions in colloid-polymer suspensions: Tests of depletion theories. *J. Chem. Phys.* **2002**, *116*, 2201-2212.

55. Peters, V. F. D.; Vis, M.; Tuinier, R.; Lekkerkerker, H. N. W. Phase separation in mixed suspensions of bacteria and nonadsorbing polymers. *J. Chem. Phys.* **2021**, *154*.

56. Tuinier, R.; Rieger, J.; de Kruif, C. G. Depletion-induced phase separation in colloid-polymer mixtures. *Adv. Colloid Interface Sci.* **2003**, *103*, 1-31.

57. Bergenholtz, J.; Poon, W. C. K.; Fuchs, M. Gelation in model colloid-polymer mixtures. *Langmuir* **2003**, *19*, 4493-4503.

58. Poon, W. C. K.; Pirie, A. D.; Pusey, P. N. Gelation in colloid-polymer mixtures. *Faraday Discuss.* **1995**, *101*, 65-76.

59. Joanny, J. F.; Leibler, L.; DeGennes, P. G. Effects of Polymer Solutions on Colloid Stability. *J. Polym. Sci. Polym Phys.* **1979**, *17*, 1073-1084.

60. Gast, A. P.; Hall, C. K.; Russel, W. B. Phase Separation Induced in Aqueous Colloidal Suspenssions by Disolved Polymer. *Faraday Discuss. Chem. Soc.* **1983**, *76*, 189-201.

61. Shave, M. K.; Balciunaite, A.; Xu, Z.; Santore, M. M. Rapid Electrostatic Capture of Rod-Shaped Particles on Planar Surfaces: Standing up to Shear. *Langmuir* **2019**, *35*, 13070-13077.